

·Electronic Supplementary Material (ESI) for Journal of Materials Chemistry A.

This journal is © The Royal Society of Chemistry 2020

Supporting Information

Enhanced Nonradical Activation of Peroxymonosulfate by Encapsulating Cobalt into Nitrogen Doped Graphene: Highlights on the Interfacial Interactions

Xiaoyong Yu,^{a,†} Lijing Wang,^{b,†} Xin Wang,^a Hongzhi Liu,^a Ziyuan Wang,^a Yixuan Huang,^a Guoqiang Shan,^a Weichao Wang,^{b*} and Lingyan Zhu^{a*}

^aMOE Key Laboratory of Pollution Processes and Environmental Criteria, Tianjin Key Laboratory of Environmental Remediation and Pollution Control, College of Environmental Science and Engineering, Nankai University, Tianjin, No. 38 Tongyan Road, Jinnan District, Tianjin, 300350, China, P.R. China

^bDepartment of Electronics, National Institute for Advanced Materials, Renewable Energy Conversion and Storage Center, Tianjin Key Laboratory of Photo-Electronic Thin Film Device and Technology, Nankai University, Tianjin 300071, China

*Corresponding authors: Weichao Wang and Lingyan Zhu

Email: weichaowang@nankai.edu.cn (W. C. Wang); zhuly@nankai.edu.cn (L. Y. Zhu)

Number of pages (including this one): 31

1 Test, 7 Tables and 22 Figures.

Table of contents

Test S1. Electrochemical analysis tests.

Test S2. The concentration procedure of samples and analysis method of UPLC-MS.

Figure S1. XRD patterns of as-synthesized ZIF-67.

Figure S2. FESEM images of ZIF-67 particles.

Figure S3. TG-DSC curves of ZIF-67.

Figure S4. SEM images of Co@NG materials.

Figure S5. (a) SEM and (b) HR-TEM images of NC-900.

Figure S6. (a) Raman spectra; and (b) I_D/I_G ratio of Co@NG materials.

Figure S7. Mass ratio of C and N elements in Co@NG materials.

Figure S8. STEM images and corresponding elemental mapping of Co@NG-900.

Figure S9. Pore size distributions of Co@NG materials.

Figure S10. XPS survey spectra and high-resolution XPS spectra of C 1s spectra of Co@NG materials.

Figure S11. Removal efficiency of phenol of Co@NG materials within 12 min.

Figure S12. Removal efficiency of phenol in different reaction systems within 12 min.

Figure S13. Removal efficiency of phenol in different reaction systems within 12 min.

Figure S14. Recycling experiments of Co@NG-900/PMS system.

Figure S15. EPR spectra of Co@NG-900/PMS system.

Figure S16. The removal of phenol and evolution of 1O_2 under different conditions;

Figure S17. Effects of quenching reagents on phenol degradation.

Figure S18. (a) The Bode plots; and (b) The Nyquist plot of Co@NG materials; (c) The Bode plots of Co@NG-900 without PMS.

Figure S19. The equivalent circuit was used.

Figure S20. Configurations of N-doped graphene

Figure S21. Configurations of graphene adsorbed on FCC-Co(111).

Figure S22. Lateral and vertical adsorption structures of PMS.

Figure S23. The relaxed top views of configurations for PMS adsorbed on different models.

Figure S24. The relaxed side views of configurations for PMS adsorbed on different models.

Figure S25. Top views of PMS adsorbed on different composite systems.

Figure S26. Work function of Co(111) and single-layer graphene.

Figure S27. Charge density differences between G and Co@G.

Table S1. The BET surface area, pore volume, pore size, chemical compositions, reaction rate constant of the as-prepared catalysts.

Table S2. Atomic percentages of nitrogen species in the as-prepared Co@NG materials.

Table S3. Atomic percentage of cobalt species for different Co@NG materials.

Table S4. The catalytic performance comparison of recently reported Fenton like catalysts for non-radical PMS activation.

Table S5. The catalytic performance comparison of recently reported Fenton like catalysts for radical PMS activation.

Table S6. The resistance (R_{ct} and R_f) of different Co@NG materials.

Table S7. The degradation products of phenol identified by UPLC-MS during the (a) Co@NG-900/PMS and (b) Co₃O₄/PMS systems.

Table S7. Adsorption energy of PMS on different models.

Table S9. HPLC analytical conditions for different organic compounds.

Test S1. Electrochemical analysis tests.

■ Preparation of activator-coated glassy carbon electrode (activator-GCE)

The suspensions were prepared by the sonication of 10 mg of activator (Co, NG or Co@NG), 0.75 mL of water, 0.20 mL of isopropanol and 0.05 mL of Nafion perfluorinated resin solution (D520, 5 wt %, DuPont) for 0.5 h. Then, the mixture (5 μ L) was dropped onto a glassy carbon electrode (Φ 5 mm) and dried for 10 min at 70 $^{\circ}$ C.

■ Analysis of linear sweep voltammetry (LSV)

Linear sweep voltammetry (LSV) was performed between 0.4 V and 1.0 V at a scan rate of 20 mV s⁻¹ on a CHI 760E electrochemical workstation. The experiments were conducted in 20 mM Na₂SO₄ solution and 1 mM chemical reagent (phenol) at pH = 7.2 with a three electrodes-cell configuration including a working electrode (activator-GCE), a counter electrode (platinum electrode, 10 \times 10 \times 0.1 mm), and a reference electrode (Ag/AgCl electrode), and all the potential values were normalized to the reversible hydrogen electrode (RHE) before testing.

■ Analysis of Tafel curve

the corresponding *Tafel* plots were constructed according to the LSV curves, and *Tafel* slope was determined by fitting LSV data to the *Tafel*

$$\eta = \varphi - \varphi_0 = a + b \log(j)$$

where η is the overpotential; φ is the electrode potential; φ_0 is the oxidation potential of phenol; j is the absolute value of current density; and a and b are the *Tafel* constant and the *Tafel* slope, respectively.

■ Chronoamperometry

Amperometric *i-t* curve was measured under the same condition as the voltammetry, but the working electrode was biased to the applied potential +0.6 V (vs Ag/AgCl), and PMS or phenol was added into solution to monitor the changed current.

■ Open circuit potential

Then the open circuit potential of activator-GCE was monitored by chronopotentiometry analysis using a Ag/AgCl electrode as the reference electrode and all the potential values were normalized to the reversible hydrogen electrode (RHE) before testing. PMS or/and phenol was added into solution to monitor the changed potential of activator-GCE after the open circuit potential keeping stable. The potential of the complex represents the stable equilibrium potential of activator (NG-900 or Co@NG-900) after adding PMS and Phenol.

Test S2. The concentration procedure of samples and analysis method of UPLC-MS.

Before the analysis of UPLC-MS, collected samples were concentrated by solid phase extraction (SPE) workstation using HLB cartridge (WAT106202, Waters Oasis). Before concentration, the cartridge was activated by 5 mL methanol, 5 mL Milli-Q water followed by 5 mL acidified deionized water (pH was adjusted to 3.0 with H₂SO₄). Then, the collected samples (50 mL), were filtered through the cartridge at a flow rate of 1 mL min⁻¹ followed by 2 mL deionized water, and 2 mL 5% aqueous methanol were employed to wash the cartridge, sequentially. And then, 2 mL methanol was employed to elute the extracts for 2-3 times. Finally, elutes were concentrated to approximately 1.0 mL with the gentle N₂ stream purging.

The intermediate products were determined by liquid chromatography-electrospray ionization mass spectrometry (LC/ESI/MS) coupled to a Xevo TQ-S triple quadrupole mass spectrometer (Waters, Milford, MA, USA). An ACQUITY C18 column (Waters, 1.7 μm, 2.1×100 mm) was used in the UPLC-Xevo TQS to separate the sample. The mobile phase of the UPLC was made up of 0.1 formic acid water (A) and 0.1 formic acid acetonitrile (B) with a gradient elution of A/B from 95/5 (v/v) to 40/60 in 12 min, decreased to 5/95 in 14 min and held for 1 min, and then changed back to 95/5 in 15.2 min and kept for 2.8 min. The flow rate was 0.3 mL/min, the column temperature was maintained at 35°C, and the injection volume was 10 μL. The ESI source was set in negative ion detection mode with the following ionization parameters: spray voltage, 2.5 kV; capillary temperature, 350°C. Full scan MS data were collected for a mass range of 50-500 amu.

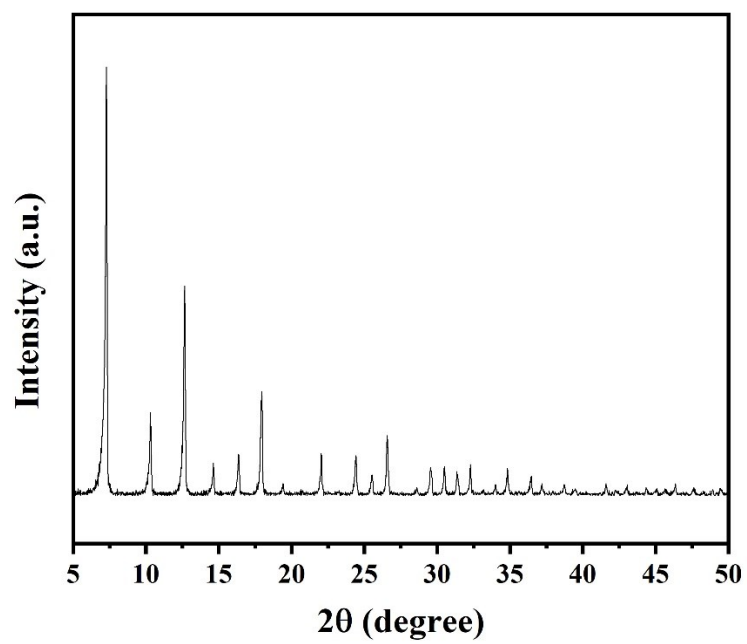


Figure S1. XRD patterns of as-synthesized ZIF-67.

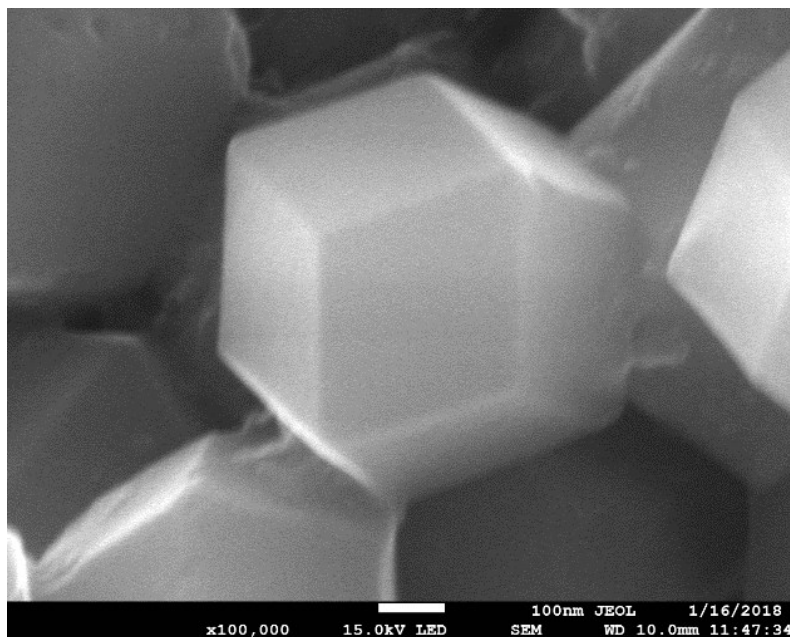


Figure S2. FESEM images of ZIF-67 particles.

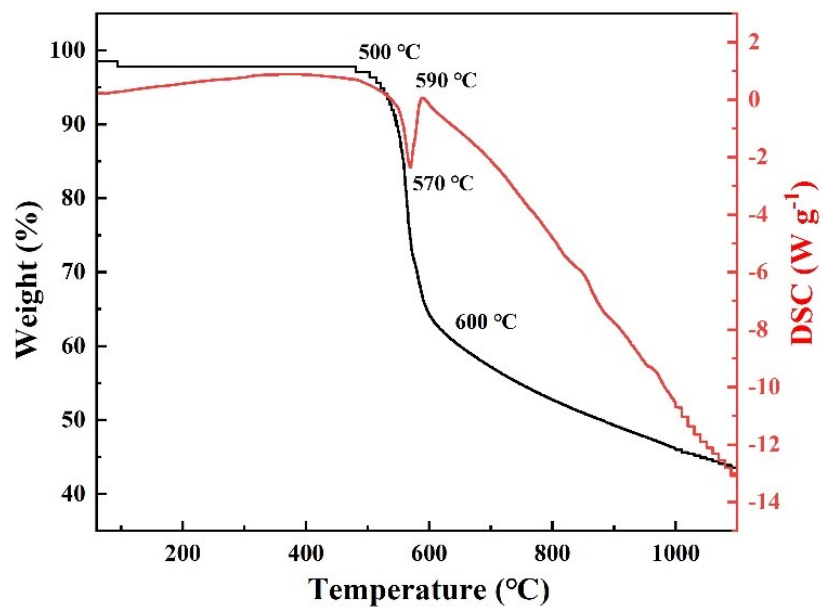


Figure S3. TG-DSC curves of ZIF-67.

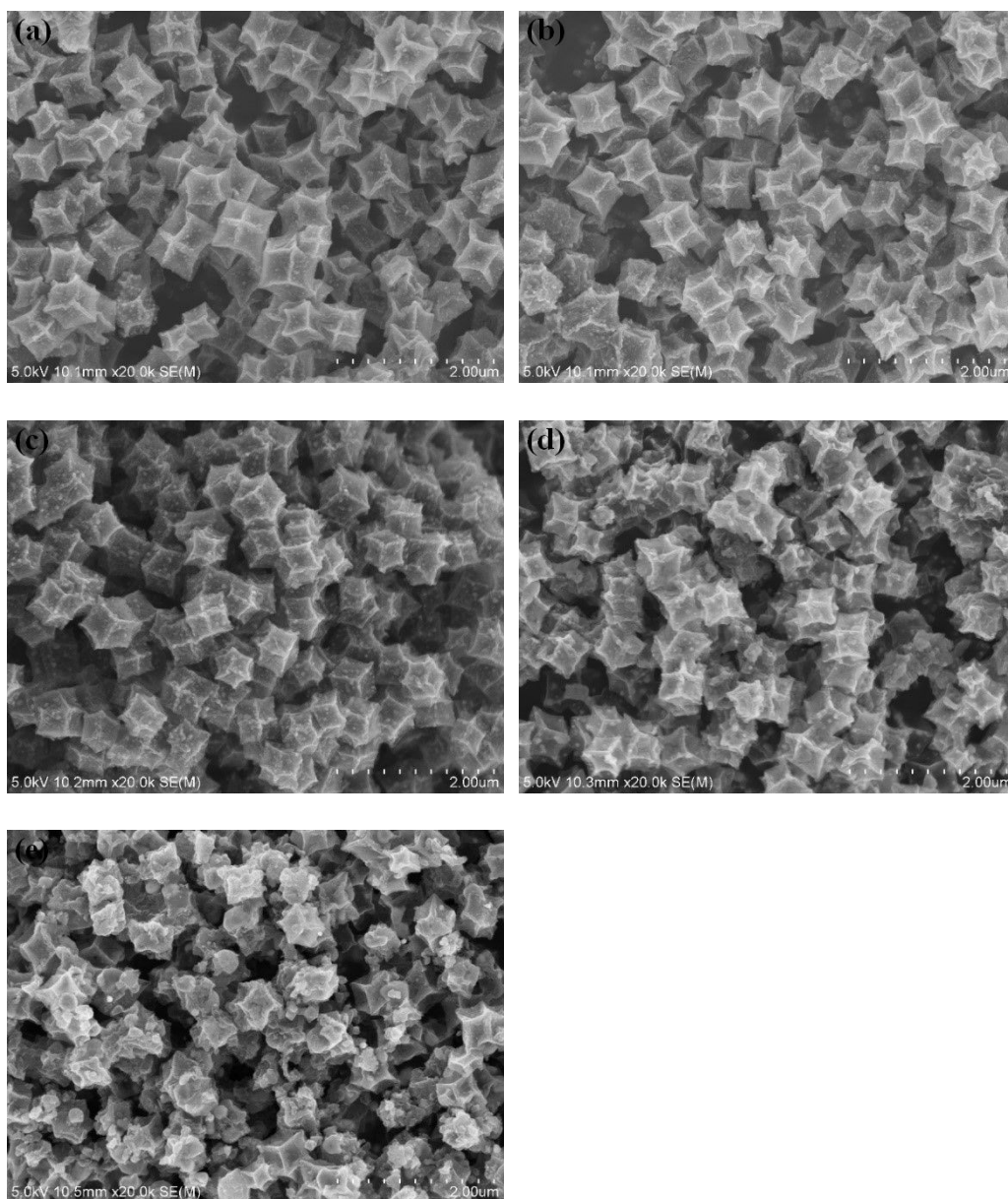


Figure S4. SEM images of (a) Co@NG-700, (b) Co@NG-800, (c) Co@NG-900, (d) Co@NG-1000, and (e) Co@NG-1100.

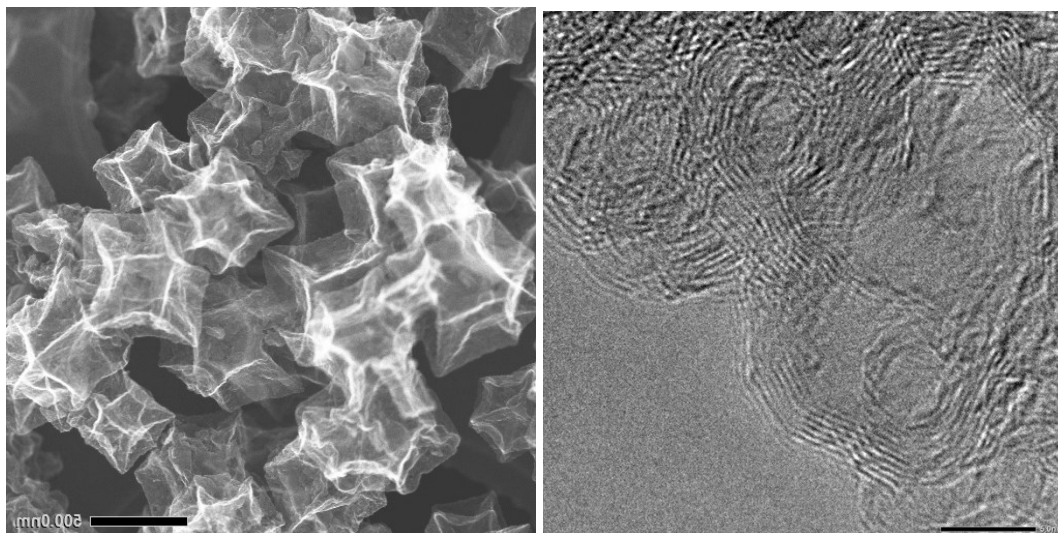


Figure S5. (a) SEM and (b) HR-TEM images of NC-900.

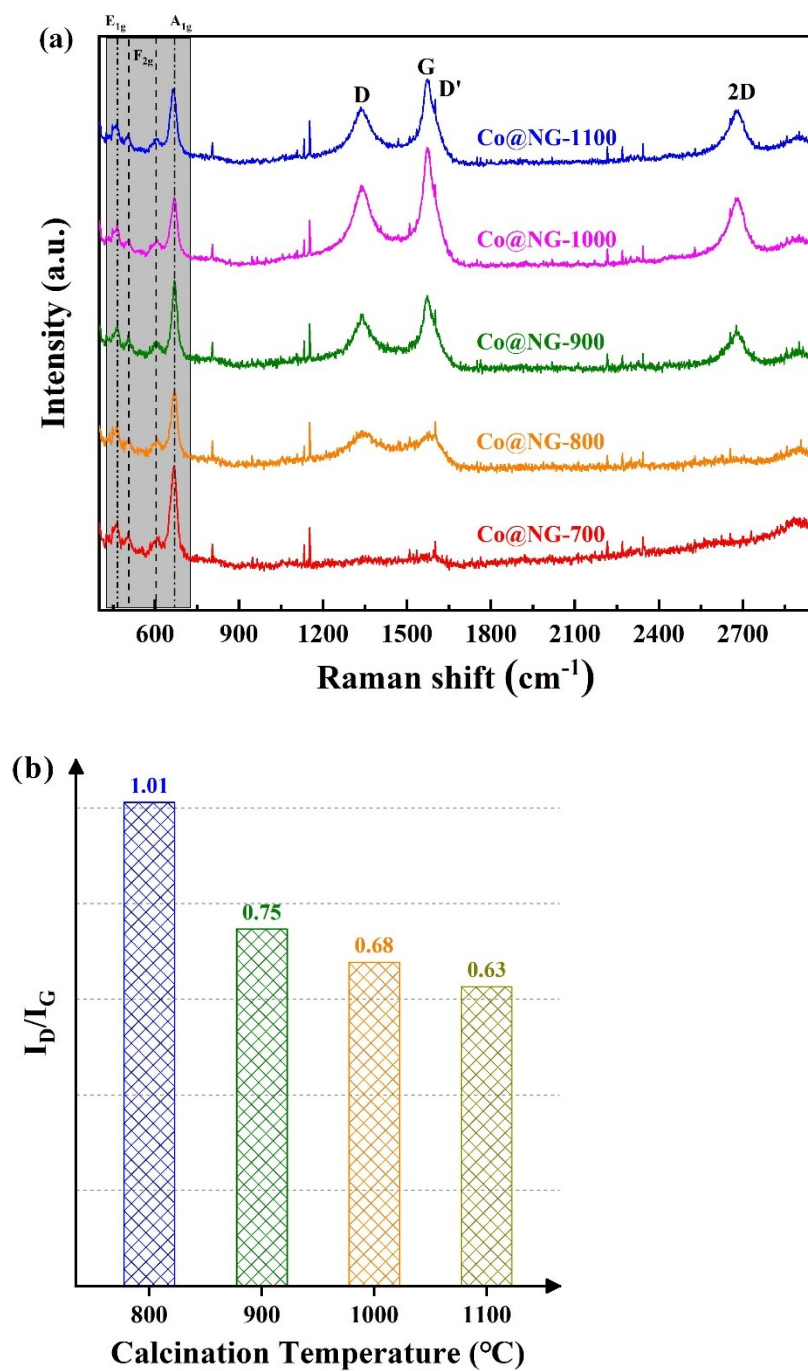


Figure S6. (a) Raman spectra; and (b) I_D/I_G ratio of Co@NG samples obtained at different calcination temperatures.

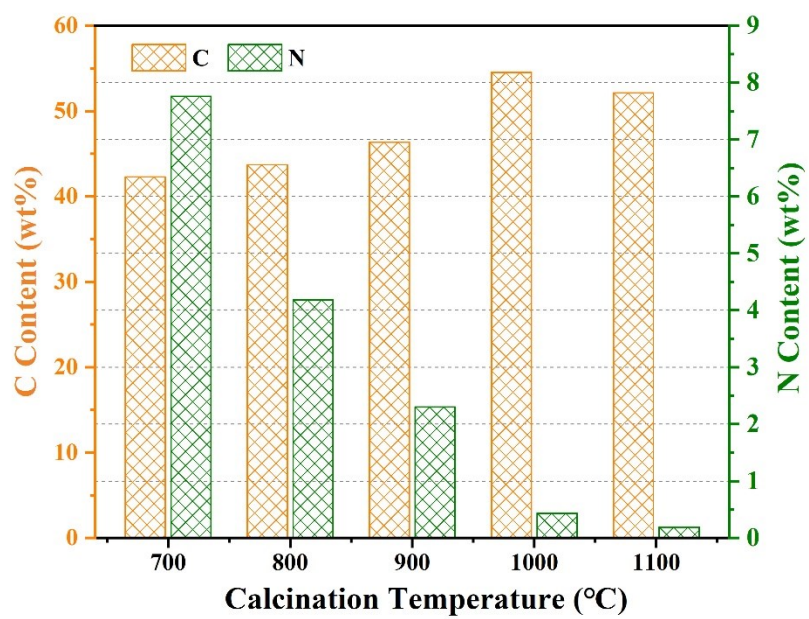


Figure S7. Mass ratio of C and N elements in Co@NG samples.

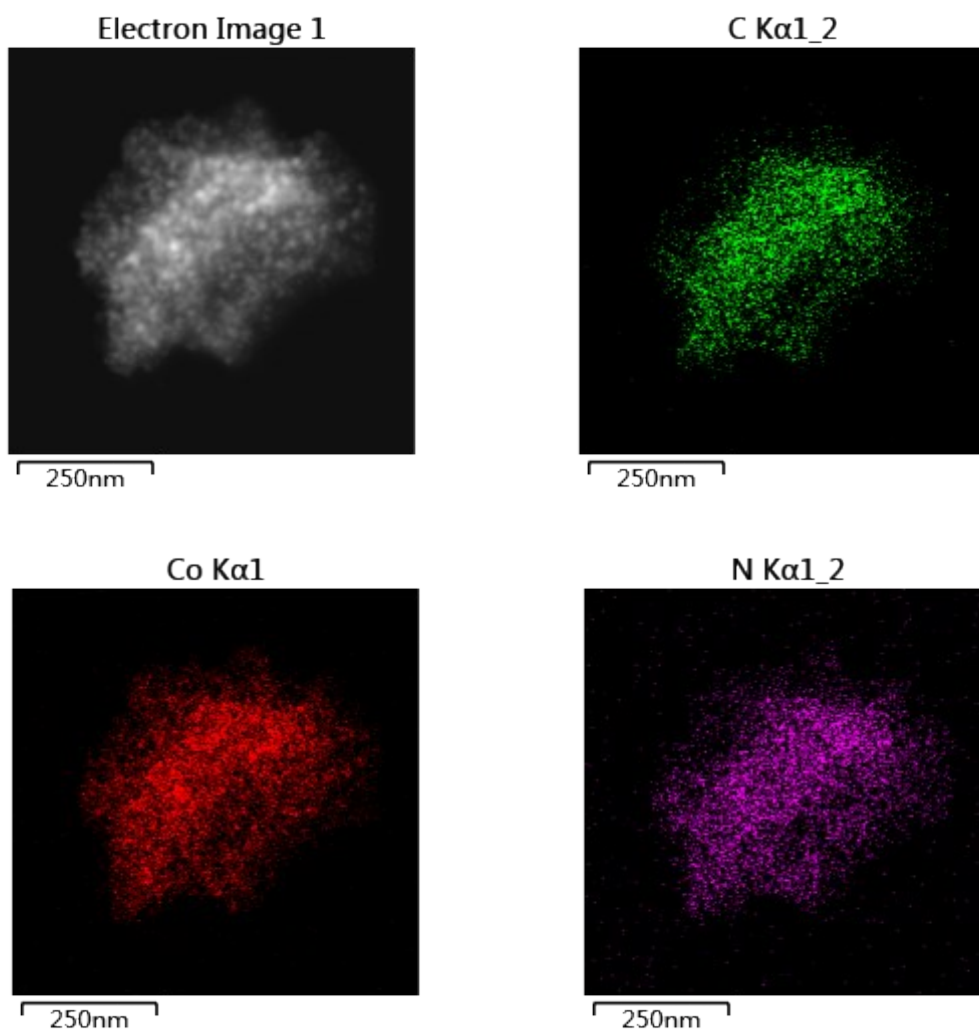


Figure S8. (a) STEM images and corresponding (b) carbon, (c) cobalt, and (d) nitrogen elemental mapping of Co@NG-900.

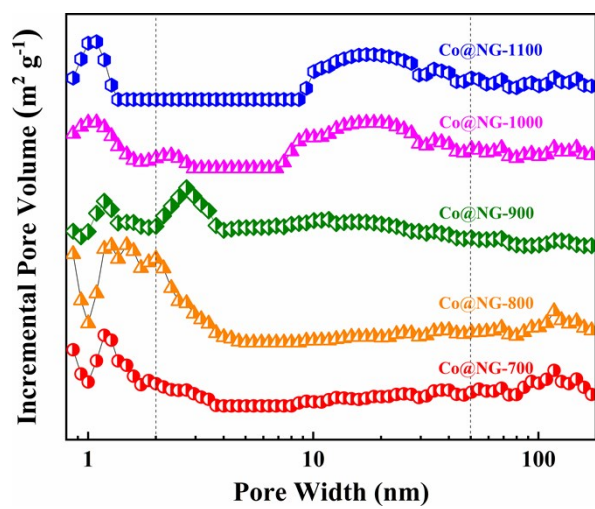


Figure S9. Pore size distributions of Co@NG materials.

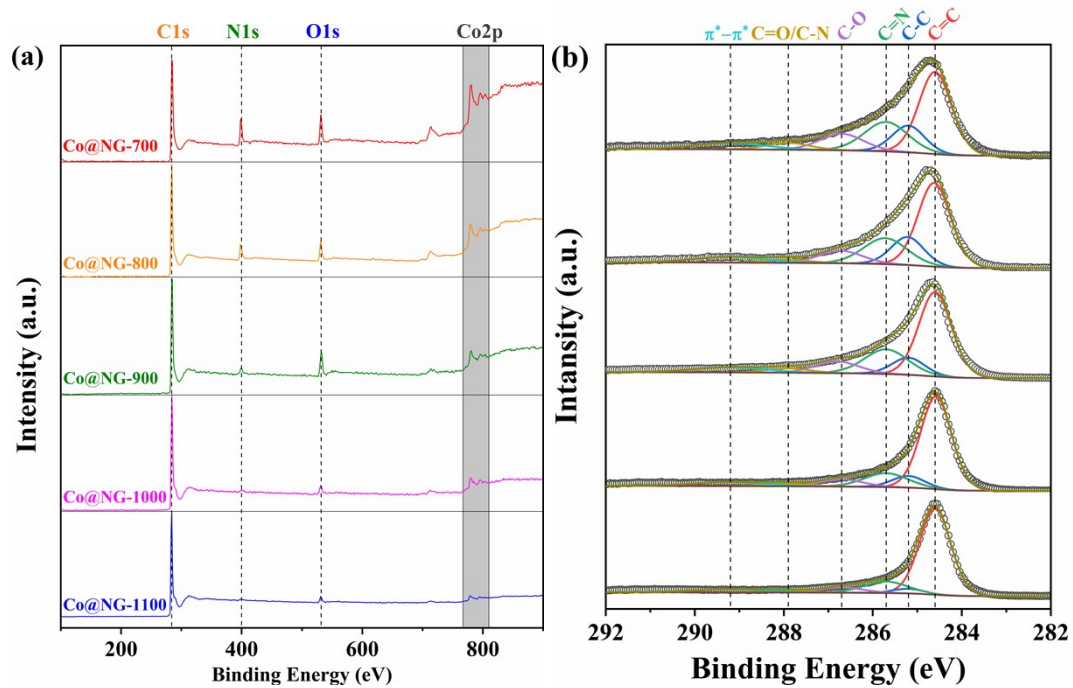


Figure S10. (a) XPS survey spectra; and (b) high-resolution XPS spectra of C 1s spectra of Co@NG materials.

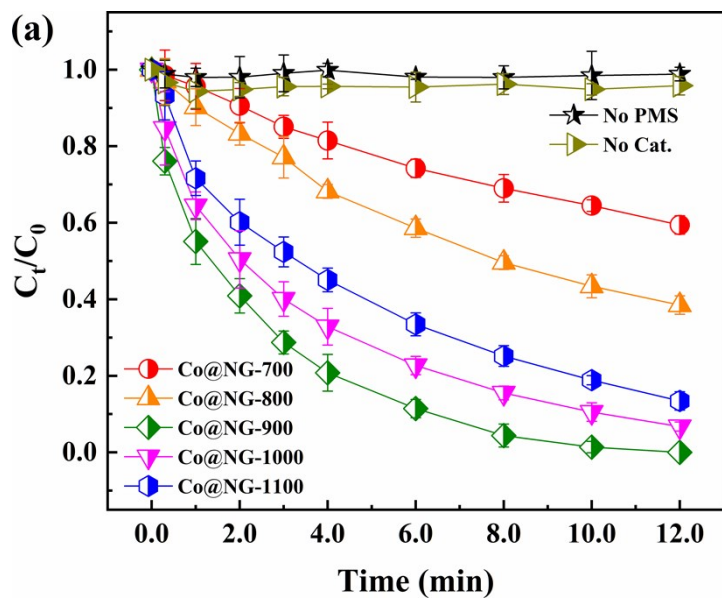


Figure S11. Removal efficiency of phenol in different reaction systems within 12 min.

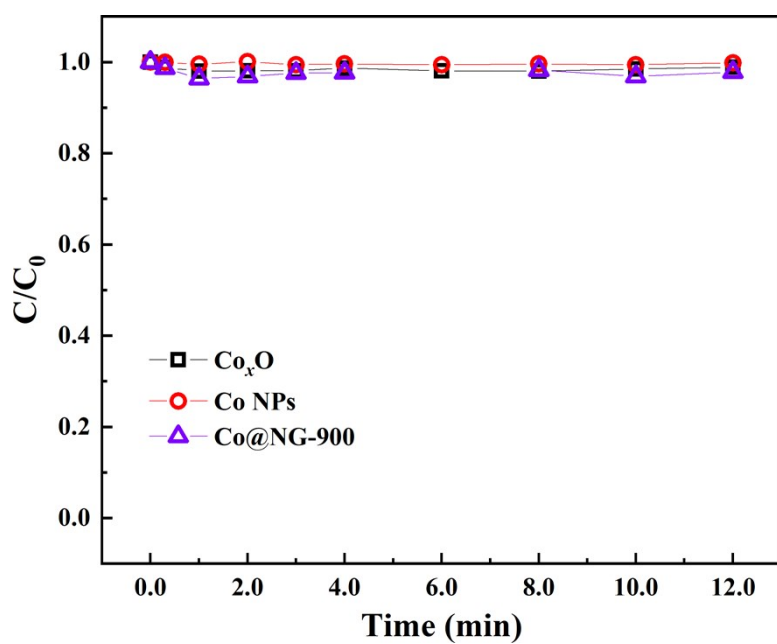
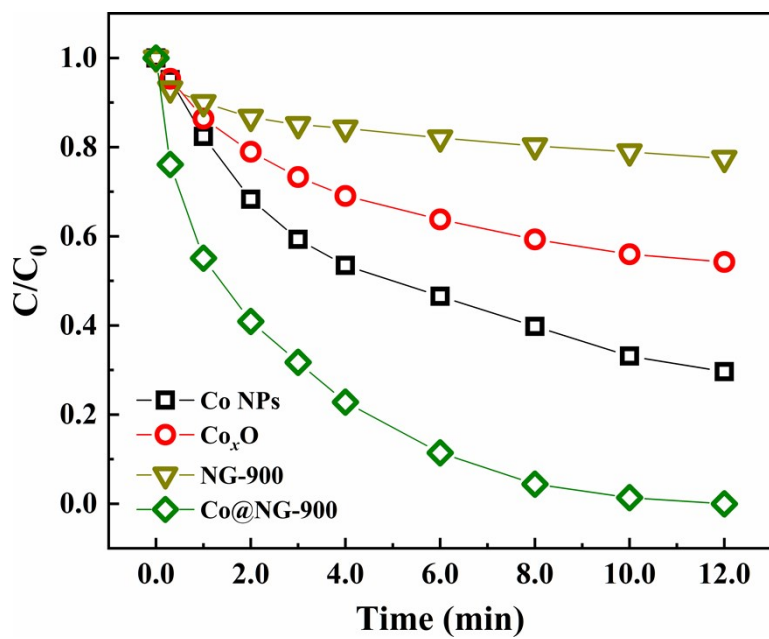


Figure S12. (a) Removal efficiency of phenol in different reaction systems within 12 min. (b)

The phenol adsorption performance of Co@NG-900, Co and Co_xO.

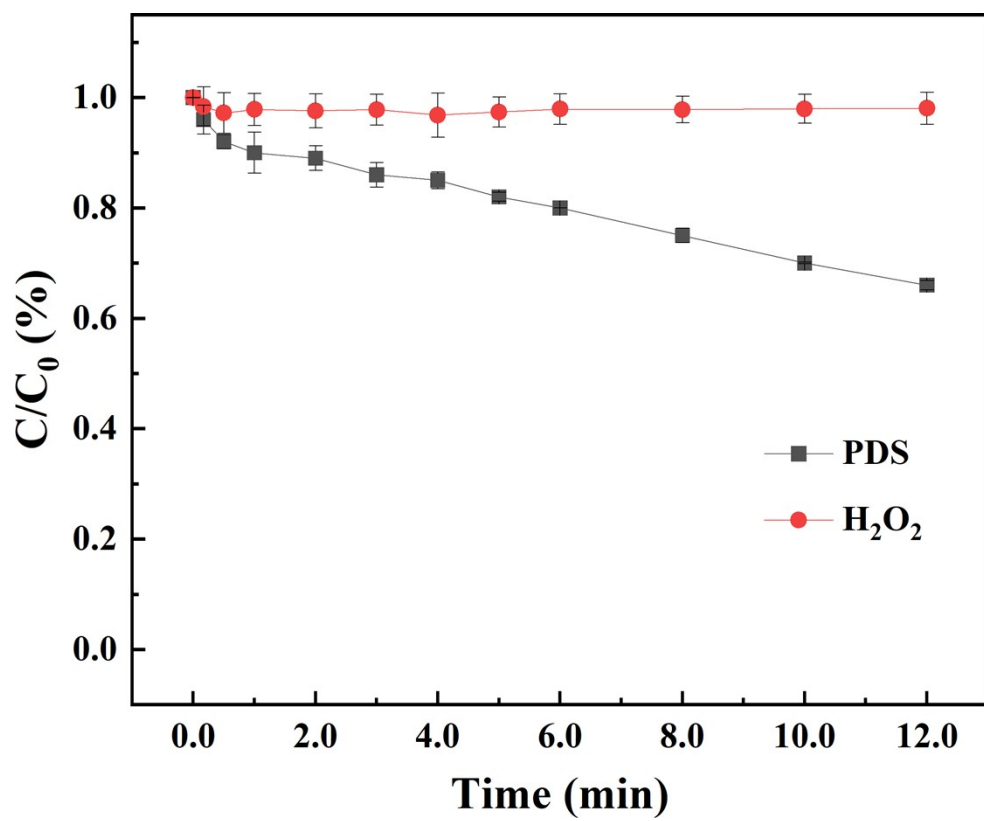


Figure S13. Removal efficiency of phenol in different reaction systems within 12 min.

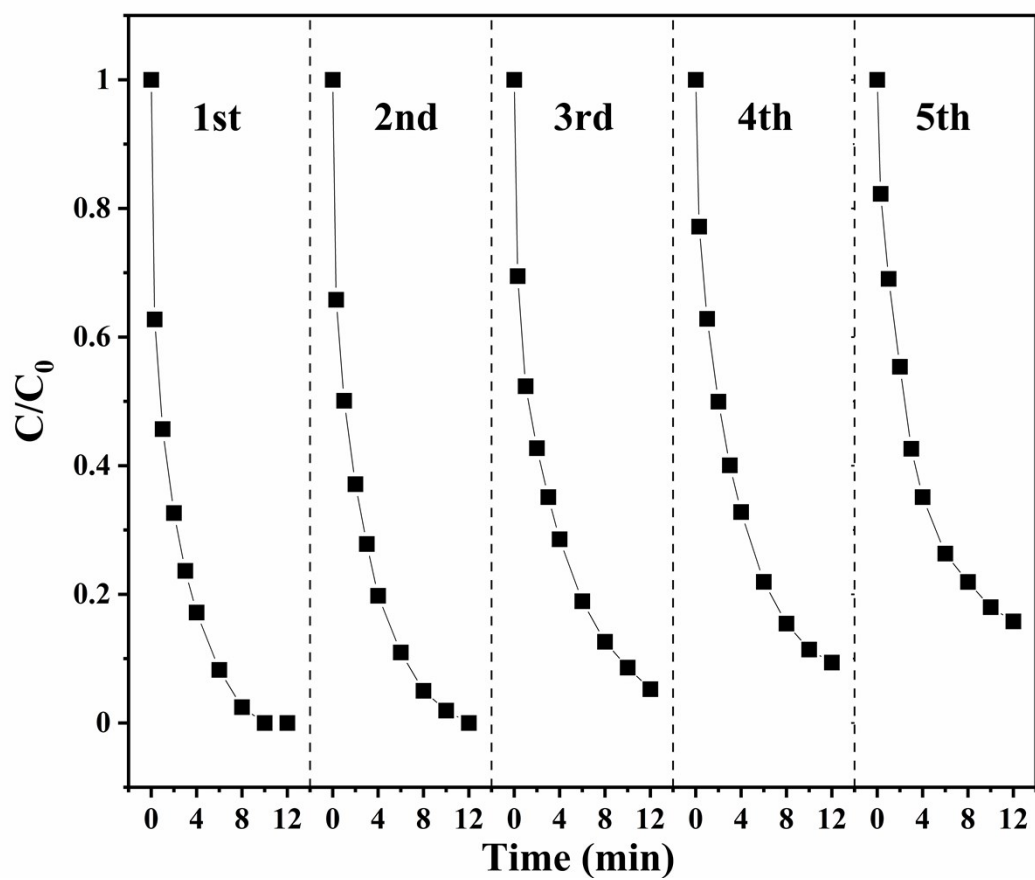


Figure S14. Recycling experiments of Co@NG-900/PMS system.

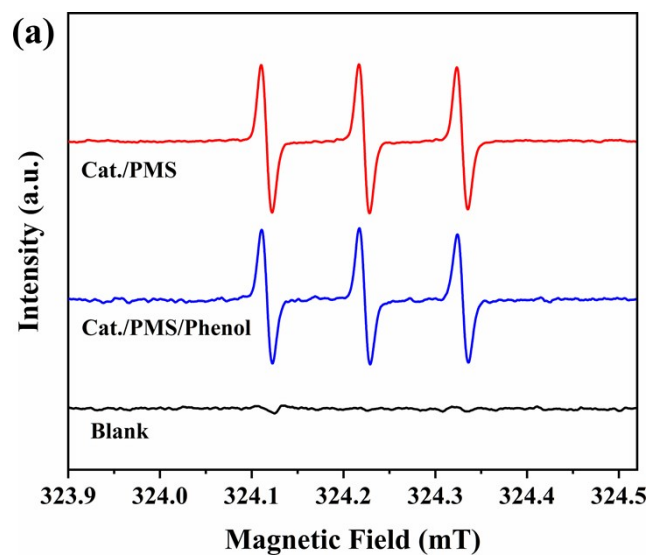


Figure S15. EPR spectra of Co@NG-900/PMS system at 3 min.

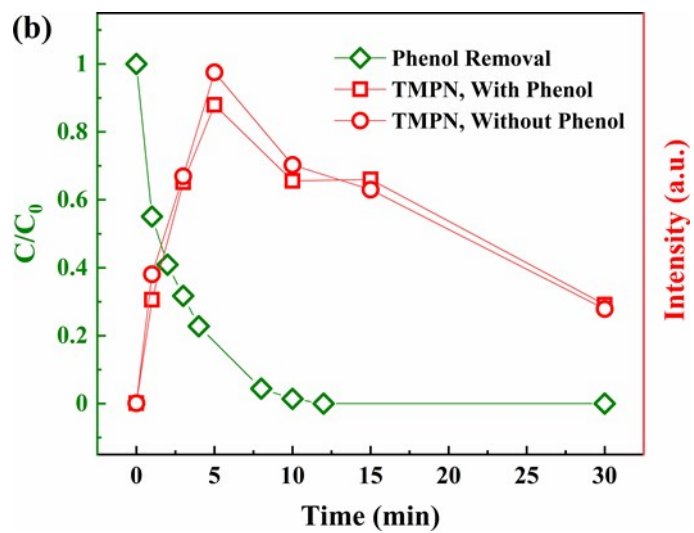


Figure S16. The removal of phenol and evolution of $^1\text{O}_2$ under different conditions.

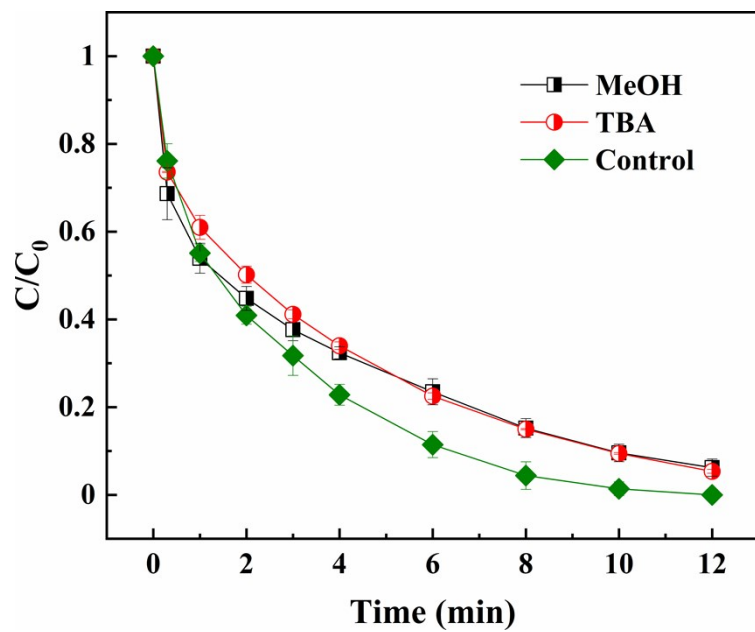


Figure S17. Effects of quenching reagents on phenol degradation.

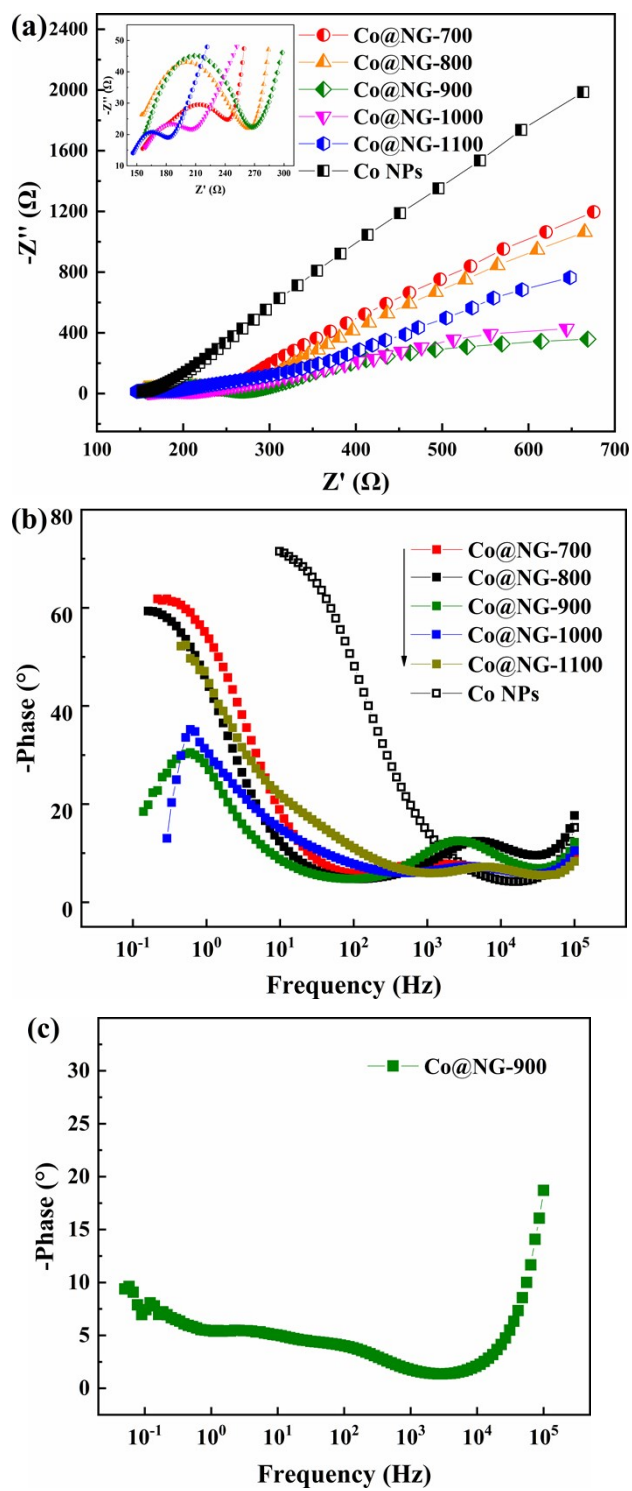


Figure S18. (a) The Bode plots; and (b) The Nyquist plot of Co@NG materials; (c) The Bode plots of Co@NG-900 without PMS.

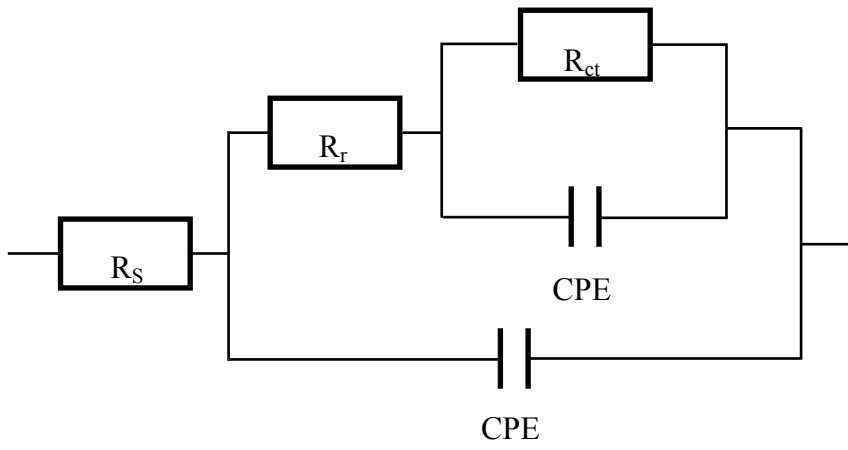


Figure S19. The equivalent circuit was used.

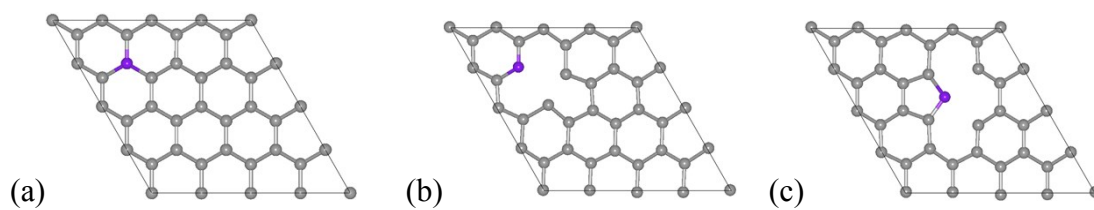


Figure S20. Configurations of N-doped graphene: (a) graphitic (b) pyridinic (c) pyrrolic.

Gray and violet atoms are C and N, respectively.

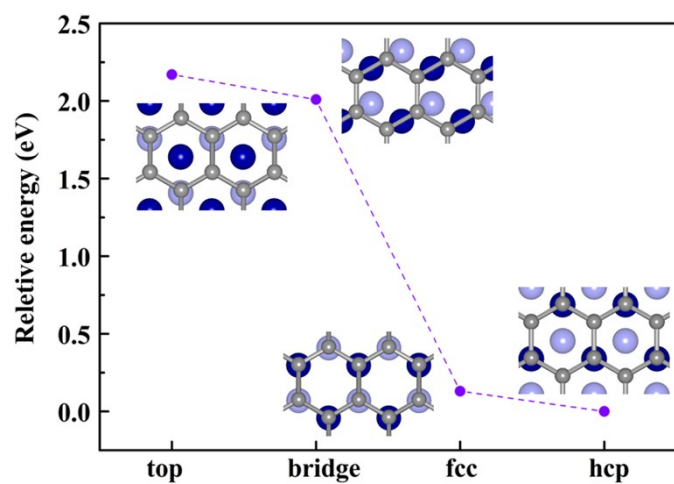


Figure S21. Configurations of graphene adsorbed on FCC-Co(111). Tests with 1x1 unit cells.

Gray atoms are graphene. Dark and light blue are the Co atoms on the surface and subsurface of Co(111).

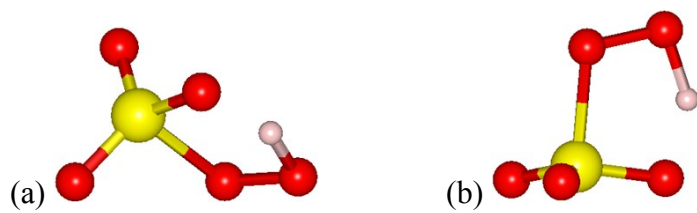


Figure S22. (a) Lateral and (b) vertical adsorption structures of PMS. The red, yellow and light pink represent O atom, S atom and H atom respectively.

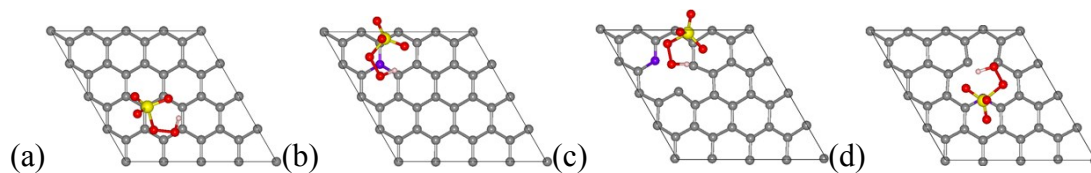


Figure S23. The relaxed top views of configurations for PMS adsorbed on different models.

(a) graphene, (b) graphitic NG, (c) pyridinic NG, and (d) pyrrolic NG. The pyrrolic NG

turned into pyridinic NG after PMS adsorbed.

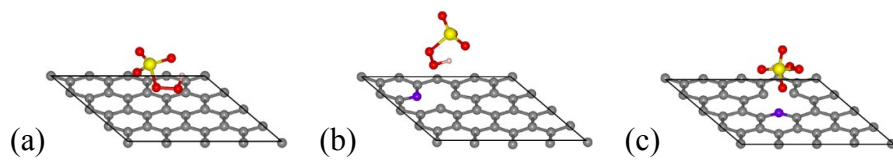


Figure S24. The relaxed side views of configurations for PMS adsorbed on different models.

(a) graphene, (b) pyridinic NG, and (c) pyrrolic NG.

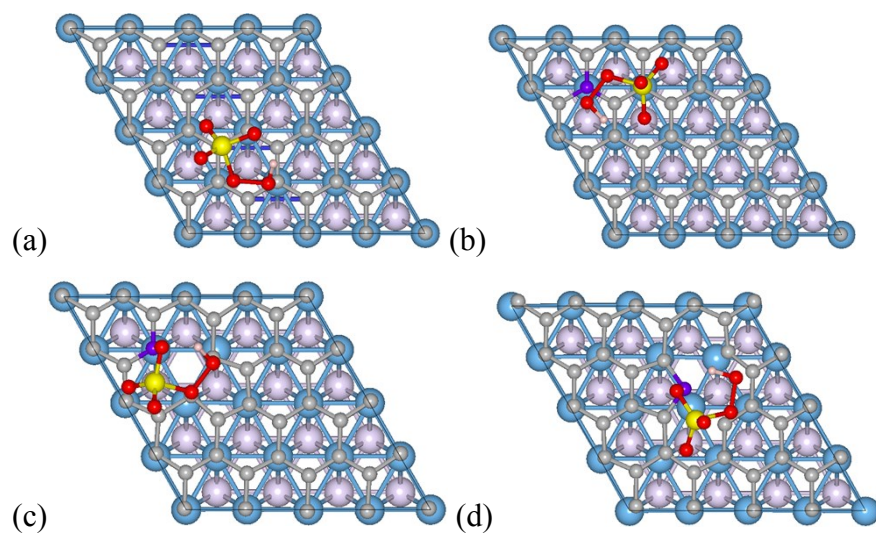


Figure S25. Top views of PMS adsorbed on different composite systems: (a) Co@G. (b) Co@graphite NG. (c) Co@pyridinic NG. (d) Co@pyrrolic NG. The blue, light violet, red, yellow and pink represent Co atom, N atom, O atom, S atom and H atom, respectively.

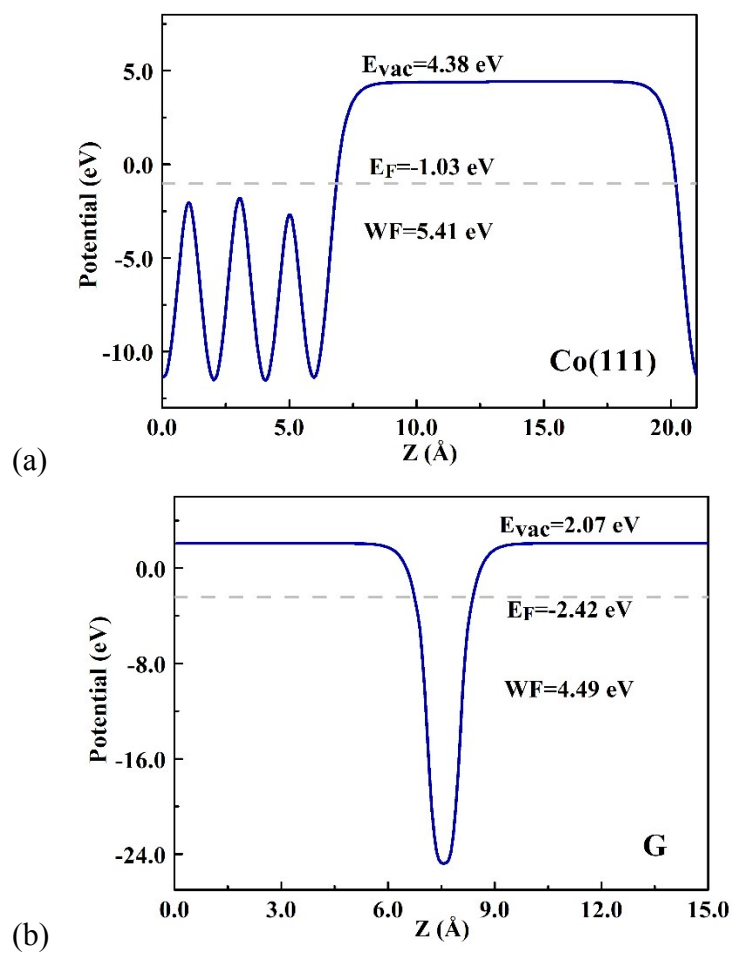


Figure S26. Work function of (a) Co(111) and (b) single-layer graphene.

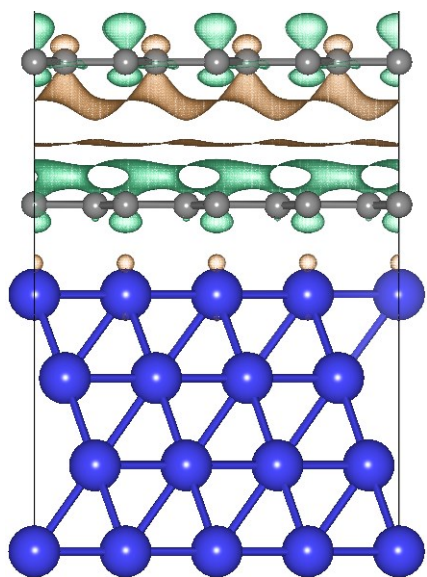


Figure S27. Charge density differences between G and Co@G. Khaki and green regions represent electron accumulation and depletion, respectively. (Isosurfaces= $0.0001e/\text{\AA}^3$)

Table S1. HPLC analytical conditions for different organic compounds.

Chemicals	Mobile phase	Volume ratio	Column	Detection wavelength
TPA	Methanol, Formic acid water (0.1 %, v/v)	60:40	Agilent Eclipse Plus–C18 (5 μ m, 150 \times 4.6 mm I.D)	240 nm
2-OH TPA	Methanol, Formic acid water (0.1 %, v/v)	60:40		Exc.: 315 nm Abs.: 435 nm
Phenol	Methanol, Acetic acid water (0.1 %, v/v)	50:50		273 nm

Table S2. The BET surface area, pore volume, pore size, chemical compositions, particles size and reaction rate constant of the as-prepared catalysts

Sample	S_{BET} ($\text{m}^2 \text{g}^{-1}$)	V_{total} ($\text{cm}^3 \text{g}^{-1}$)	Pore size (\AA)	C content (wt%)	N content (wt%)	particles size	k (min^{-1})	R^2	k' ($\text{min}^{-1} \text{m}^{-2} \text{g}$)
ZIF-67	1762.2	0.66	1.50	43.0	25.3	—	—	—	—
Co@NG-700	378.1	0.23	2.44	42.3	13.6	6~21 nm	0.045	0.99	0.119×10^{-3}
Co@NG-800	273.9	0.18	2.66	43.7	9.0	6~24 nm	0.084	1.00	0.353×10^{-3}
Co@NG-900	139.4	0.16	4.49	46.4	4.0	6~30 nm	0.397	0.99	2.848×10^{-3}
Co@NG-1000	88.7	0.11	4.95	54.5	2.5	15~42 nm	0.218	0.98	2.458×10^{-3}
Co@NG-1100	71.6	0.10	5.38	52.1	0.9	30~200 nm	0.161	0.98	2.249×10^{-3}
NG-900	344.3	0.58	6.72	96.2	3.8	—	0.019	0.96	0.055×10^{-3}
Co_xO	54.3	0.75	2.32	—	—	6~15 nm	0.056	0.92	—
Co NPs	5.2	—	—	—	—	300 目	0.107	0.95	—

Table S3. Atomic percentages of nitrogen species in the as-prepared Co@NG materials.

Sample	N1 (at. %)	N-Co (at. %)	N2 (at. %)	G-N (at. %)	O-N (at. %)
Co@NG-700	7.2	2.2	2.6	0.2	1.2
Co@NG-800	4.3	1.3	2.3	0.3	0.8
Co@NG-900	1.2	0.9	1.3	0.5	0.7
Co@NG-1000	0.7	0.2	0.7	0.6	0.4
Co@NG-1100	0.2	0.1	0.2	0.3	0.1

Table S4. Atomic percentage of cobalt species for different Co@NG materials.

Sample	Co ⁰ (at. %)	CoC _x N _x (at. %)	CoN _x (at. %)
Co@NG-700	11.5	67.7	20.6
Co@NG-800	4.2	72.8	23.0
Co@NG-900	6.2	76.7	17.1
Co@NG-1000	12.3	72.7	14.9
Co@NG-1100	22.3	62.4	15.3

Table S5. The catalytic performance comparison of recently reported Fenton like catalysts for non-radical PMS activation. The turnover frequency (TOF) was calculated through dividing the reaction rate of pollutant degradation by the catalyst concentration.¹

Catalyst (g L ⁻¹)	PMS (mM)	Pollutant	Con. (mM)	Removal efficiency	k_{obs} (min ⁻¹)	TOF (g ⁻¹ min ⁻¹)	Ref.
S-ND-900 (0.1)	6.5	Phenol	0.21	100% (90 min)	0.030	0.30	2
N-rGO (0.4)	6.5	Phenol	0.21	100% (20 min)	0.400	1.00	3
NC-900 (0.1)	3.3	Phenol	0.21	100% (120 min)	~0.028	~0.28	4
Cu ₂ O (0.2)	1.0	Phenol	0.04	—	~0.024	~0.12	5
N-CNT-700 (0.1)	6.5	Phenol	0.21	100% (20min)	0.247	2.47	6
Fe ₃ C@NCNT-900 (0.2)	6.5	Phenol	0.21	100% (20 min)	0.330	1.65	7
N-CNT-B1 (0.1)	0.2	Phenol	0.10	100% (4 min)	0.227	2.27	8
Fe _{0.15} Mn _{0.85} O ₂ (0.04)	0.5	MB	0.04	100% (20 min)	0.074	1.85	9
NC1.0 (0.2)	2.0	BPA	0.01	100% (15min)	0.260	1.30	10
Fe-Mn-O (0.5)	0.6	BPA	0.04	100% (25min)	0.295	0.59	11
MnO ₂ (0.02)	0.4	BPA	0.04	100% (60 min)	0.018	0.90	12
AND-800 (0.1)	0.3	4-CP	0.16	100% (45min)	0.122	1.22	13
CNT (0.1)	1.0	4-CP	0.10	100% (30 min)	0.015	0.15	14
CNT (0.1)	1.0	4-CP	0.05	100% (20 min)	~0.200	~2.00	15
CuOMgO/Fe ₃ O ₄ (0.2)	2.0	4-CP	0.31	100% (20 min)	0.162	0.81	16
O-CNTs-1000 (0.1)	0.5	4-CP	0.16	100% (60 min)	0.096	0.96	17
Co@NG-900 (0.05)	3.0	Phenol	1.00	100% (12 min)	0.397	7.94	This work

Table S6. The catalytic performance comparison of recently reported Fenton like catalysts for radical PMS activation.

Catalyst (g L ⁻¹)	PMS (mM)	Pollutant	Con. (mM)	Removal efficiency	<i>k</i> _{obs} (min ⁻¹)	TOF (g ⁻¹ min ⁻¹)	Ref
MnO ₂ /ZnFe ₂ O ₄ (0.2)	13	Phenol	0.21	100% (120 min)	0.032	0.16	18
MnO ₂ nanorods (0.2)	13	Phenol	0.21	100% (30 min)	0.148	0.74	19
NC ZIF-8 (0.2)	3.3	Phenol	0.21	100% (60 min)	0.078	0.39	20
CuFe ₂ O ₄ -Fe ₂ O ₃ (0.2)	2.6	BPA	0.02	100% (10 min)	0.620	3.10	21
CoO _x -C (0.1)	0.3	Phenol	0.21	100% (60 min)	0.130	1.30	22
Mn _{1.8} Fe _{1.4} O ₄ (0.1)	1.3	BPA	0.04	95% (30 min)	0.102	1.02	23
Fe ³⁺ -g C ₃ N ₄ (0.1)	2.0	BPA	0.10	100% (15 min)	0.302	3.02	24
Fe ₃ Co ₇ @C (0.1)	1.3	BPA	0.09	95% (30 min)	0.132	1.32	25
Fe ₃ O ₄ -MnO ₂ -ZIF-8 (0.5)	2.0	BPA	0.26	93% (15 min)	0.428	0.86	26
CoNi ₃ O ₄ @Diatomite (0.1)	0.3	ATZ	0.02	93% (30 min)	0.084	0.84	27
Co-S@NC (0.1)	0.65	DIN	0.05	10% (90 min)	0.048	0.48	28
AgFeO ₂ (0.1)	0.02	OI	0.01	88% (30 min)	0.068	0.68	29
FeSe ₂ (0.5)	1.0	BPA	0.09	95% (60 min)	0.024	0.05	30
LaBaCoMnO (0.1)	6.5	Phenol	0.27	100% (30 min)	0.130	1.30	31
Boron (0.2)	3.0	DEP	0.01	95% (60 min)	0.051	0.255	32
Co-SAs (0.2)	2.6	BPA	0.88	82% (12 min)	0.157	0.785	33

Table S7. The resistance (R_{ct} and R_r) of different Co@NG materials.

Sample	R_r (k Ω)	R_{ct} (Ω)	χ^2
Co@NG-700	16.4	143	0.16
Co@NG-800	14.9	176	1.34
Co@NG-900	0.91	153	0.29
Co@NG-1000	1.19	114	0.68
Co@NG-1100	4.24	86	0.79

Table S8. The degradation products of phenol identified by UPLC-MS during the (a) Co@NG-900/PMS and (b) Co_xO/PMS systems.

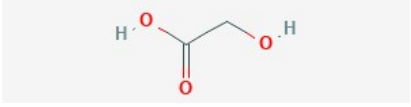
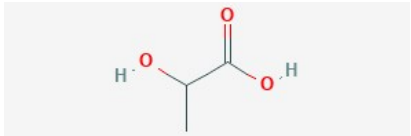
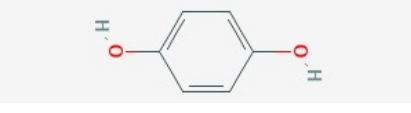
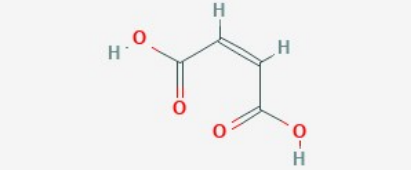
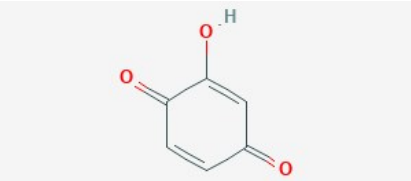
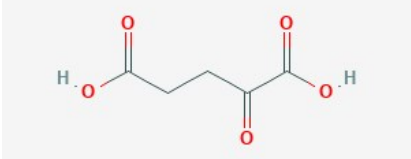
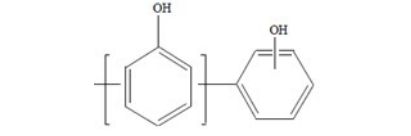
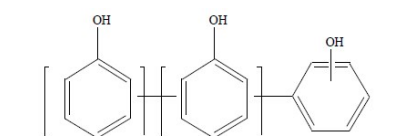
No.	Compounds	Chemical Formula	Catalysts		m/z	Molecular structure
			Co@NG	Co _x O		
1	Glycolic acid	C ₂ H ₄ O ₃	◇	●	75	
2	Lactic acid	C ₃ H ₆ O ₃	●	●	89	
3	Benzoquinone	C ₆ H ₄ O ₂	●	●	107	
4	Hydroquinone	C ₆ H ₆ O ₂	●	●	109	
5	Maleic acid	C ₄ H ₄ O ₄	●	●	115	
6	Hydroxyquinol	C ₆ H ₆ O ₃	◇	●	125	
6	Ketoglutaric acid	C ₅ H ₆ O ₅	●	●	145	
7	Biphenol	C ₁₂ H ₁₀ O ₂	●	◇	185	
8	Triphenol	C ₁₈ H ₁₄ O ₃	●	◇	277	

Table S9. Adsorption energy of PMS on different models. E_{ad1} and E_{ad2} represent the lateral and vertical adsorption, respectively.

	E_{ad1} (eV)	E_{ad2} (eV)
free PMS	-	-
G	-0.92	-0.95
graphitic NG	-1.99	-1.93
pyridinic NG	-1.11	-0.85
pyrrolic NG	-1.14	-0.88
Co	-	-3.16

References

1. X. Li, X. Huang, S. Xi, S. Miao, J. Ding, W. Cai, S. Liu, X. Yang, H. Yang, J. Gao, J. Wang, Y. Huang, T. Zhang and B. Liu, *J Am Chem Soc*, 2018, 140, 12469-12475.
2. X. Duan, Z. Ao, H. Zhang, M. Saunders, H. Sun, Z. Shao and S. Wang, *Applied Catalysis B: Environmental*, 2018, 222, 176-181.
3. D. Li, X. Duan, H. Sun, J. Kang, H. Zhang, M. O. Tade and S. Wang, *Carbon*, 2017, 115, 649-658.
4. P. Hu, H. Su, Z. Chen, C. Yu, Q. Li, B. Zhou, P. J. J. Alvarez and M. Long, *Environ Sci Technol*, 2017, 51, 11288-11296.
5. H. Li, J. Tian, F. Xiao, R. Huang, S. Gao, F. Cui, S. Wang and X. Duan, *Journal of Hazardous Materials*, 2020, 385, 121518.
6. X. Duan, H. Sun, Y. Wang, J. Kang and S. Wang, *Acs Catal*, 2015, 5, 553-559.
7. C. Wang, J. Kang, P. Liang, H. Zhang, H. Sun, M. O. Tade and S. Wang, *Environmental Science: Nano*, 2017, 4, 170-179.
8. W. Ren, G. Nie, P. Zhou, H. Zhang, X. Duan and S. Wang, *Environ Sci Technol*, 2020, 54, 6438-6447.
9. K. Z. Huang and H. Zhang, *Environ Sci Technol*, 2019, 53, 12610-12620.
10. Y. Gao, T. Li, Y. Zhu, Z. Chen, J. Liang, Q. Zeng, L. Lyu and C. Hu, *Journal of Hazardous Materials*, 2020, 393, 121280.
11. L. Yu, G. Zhang, C. Liu, H. Lan, H. Liu and J. Qu, *Acs Catal*, 2018, 8, 1090-1096.
12. L. Wang, J. Jiang, S.-Y. Pang, Y. Zhou, J. Li, S. Sun, Y. Gao and C. Jiang, *Chemical Engineering Journal*, 2018, 352, 1004-1013.
13. P. Shao, J. Tian, F. Yang, X. Duan, S. Gao, W. Shi, X. Luo, F. Cui, S. Luo and S. Wang, *Adv Funct Mater*, 2018, 28, 1705295.
14. E.-T. Yun, H.-Y. Yoo, H. Bae, H.-I. Kim and J. Lee, *Environ Sci Technol*, 2017, 51, 10090-10099.
15. E.-T. Yun, J. H. Lee, J. Kim, H.-D. Park and J. Lee, *Environ Sci Technol*, 2018, 52, 7032-7042.

16. A. Jawad, K. Zhan, H. Wang, A. Shahzad, Z. Zeng, J. Wang, X. Zhou, H. Ullah, Z. Chen and Z. Chen, *Environ Sci Technol*, 2020, 54, 2476-2488.
17. P. Shao, S. Yu, X. Duan, L. Yang, H. Shi, L. Ding, J. Tian, L. Yang, X. Luo and S. Wang, *Environ Sci Technol*, 2020, 54, 8464-8472.
18. W.-D. Oh, Z. Dong and T.-T. Lim, *Applied Catalysis B: Environmental*, 2016, 194, 169-201.
19. Y. Wang, S. Indrawirawan, X. Duan, H. Sun, H. M. Ang, M. O. Tadé and S. Wang, *Chemical Engineering Journal*, 2015, 266, 12-20.
20. G. Wang, S. Chen, X. Quan, H. Yu and Y. Zhang, *Carbon*, 2017, 115, 730-739.
21. W.-D. Oh, Z. Dong, Z.-T. Hu and T.-T. Lim, *Journal of Materials Chemistry A*, 2015, 3, 22208-22217.
22. Y. Wang, D. Cao and X. Zhao, *Chemical Engineering Journal*, 2017, 328, 1112-1121.
23. G.-X. Huang, C.-Y. Wang, C.-W. Yang, P.-C. Guo and H.-Q. Yu, *Environ Sci Technol*, 2017, 51, 12611-12618.
24. H. Li, C. Shan and B. Pan, *Environ Sci Technol*, 2018, 52, 2197-2205.
25. X. Li, A. I. Rykov, B. Zhang, Y. Zhang and J. Wang, *Catalysis Science & Technology*, 2016, 6, 7486-7494.
26. L. Dong, Y. Li, D. Chen, X. Chen and D. Zhang, *ACS ES&T Water*, 2020, DOI: 10.1021/acsestwater.0c00169.
27. X. Dong, B. Ren, X. Zhang, X. Liu, Z. Sun, C. Li, Y. Tan, S. Yang, S. Zheng and D. D. Dionysiou, *Applied Catalysis B: Environmental*, 2020, 272, 118971.
28. W. Du, Q. Zhang, Y. Shang, W. Wang, Q. Li, Q. Yue, B. Gao and X. Xu, *Applied Catalysis B: Environmental*, 2020, 262, 118302.
29. Y. Zhao, H. An, J. Feng, Y. Ren and J. Ma, *Environ Sci Technol*, 2019, 53, 4500-4510.

30. G. Fang, T. Zhang, H. Cui, D. D. Dionysiou, C. Liu, J. Gao, Y. Wang and D. Zhou, *Environ Sci Technol*, 2020, 54, 15489-15498.
31. Y. Wang, Z. Chi, C. Chen, C. Su, D. Liu, Y. Liu, X. Duan and S. Wang, *Applied Catalysis B: Environmental*, 2020, 272, 118972.
32. W. Ren, P. Zhou, G. Nie, C. Cheng, X. Duan, H. Zhang and S. Wang, *Water Res*, 2020, 186, 116361.
33. Y. Gao, C. Yang, M. Zhou, C. He, S. Cao, Y. Long, S. Li, Y. Lin, P. Zhu and C. Cheng, *Small*, 2020, 16, 2005060.